

## Article

# Settlement Relevant Load Combinations and Force Redistribution in Structural Design

Christian Wallner <sup>1,\*</sup>, Jakob Resch <sup>2</sup> and Dirk Schlicke <sup>1</sup><sup>1</sup> Institute of Structural Concrete, Technical University Graz, 8010 Graz, Austria; dirk.schlicke@tugraz.at<sup>2</sup> IKK Group, Reininghausstraße 78, 8020 Graz, Austria; jakob.resch@ikkgroup.at

\* Correspondence: christian.wallner@tugraz.at

## Abstract

Settlement-relevant load combinations play a critical role in the serviceability design of buildings, particularly for structures on soils with time-dependent deformation behavior. While permanent loads must be fully considered, the contribution of variable actions depends on their duration relative to soil response. This study investigates suitable settlement-relevant load combinations and their influence on the restrained load redistribution within buildings, based on parametric finite element analyses of wall-type and frame-type structures on sand, silt, and clay using PLAXIS 3D (Version 2024.3). Results show that structural stiffness significantly affects force redistribution due to settlements: stiffer structures exhibit greater redistribution, while soft soils generate higher absolute restraining forces but are less sensitive to load combinations. Based on these findings, the reduced characteristic load combination (including  $\alpha_n$ ) is recommended for coarse-grained, drained soils, as it balances safety and realistic deformation. For fine-grained, low-permeability soils, the quasi-permanent combination should be applied to capture long-term consolidation effects. Short-term load variations after consolidation have negligible impact and should be addressed through safety factors rather than separate settlement analyses. These recommendations provide a clear and practical framework for selecting settlement-relevant load combinations, enhancing reliability and efficiency in structural design.

**Keywords:** soil–structure interaction; nonlinear soil modeling; settlement relevant load combination; FEM; structural design



Academic Editors: Nerio Tullini and Yong Tan

Received: 14 August 2025

Revised: 8 September 2025

Accepted: 3 October 2025

Published: 7 October 2025

**Citation:** Wallner, C.; Resch, J.; Schlicke, D. Settlement Relevant Load Combinations and Force Redistribution in Structural Design. *Buildings* **2025**, *15*, 3596. <https://doi.org/10.3390/buildings15193596>

**Copyright:** © 2025 by the authors. Licensee MDPI, Basel, Switzerland. This article is an open access article distributed under the terms and conditions of the Creative Commons Attribution (CC BY) license (<https://creativecommons.org/licenses/by/4.0/>).

## 1. Introduction

Settlement-relevant load combinations play a critical role in the serviceability design of buildings, particularly on soils with time-dependent deformation behavior. While existing studies have defined appropriate combinations of permanent and variable actions, little attention has been given to their effect on internal force redistribution within the superstructure (Figure 1). This study addresses this gap by investigating how different load combinations influence force redistribution when applied through a representative settlement trough.

Various approaches can be found in the literature regarding appropriate load assumptions for settlement analysis. Across all reviewed sources, there is consensus that permanent actions, particularly the self-weight of the structure, should be fully considered, whereas variable actions such as imposed or live loads should only be considered to a limited extent. In this regard, Eurocode EN 1990 [1] provides a valuable framework through its classification of rare, frequent, and quasi-permanent load combinations, each associated

with combination factors  $\psi_0$ ,  $\psi_1$ , and  $\psi_2$ . These factors account for the probability and persistence of variable actions. Based on these assumptions, [2] is recommending the quasi permanent load combination for fine grained soils and together with [3] the frequent load combination for coarse grained soils. In [4,5] it is suggested to take the dead load and only the permanent live load proportion into account, but it's not described in detail what should be considered as permanent live load. In [6] a factor of 0.1–0.2 is applied on the variable loads whereas [7] suggest 0.7 as factor. Fischer [8] recommends the quasi-permanent load combination in general including a quasi-permanent wind component of 0.2 as settlement relevant for slim, high buildings.

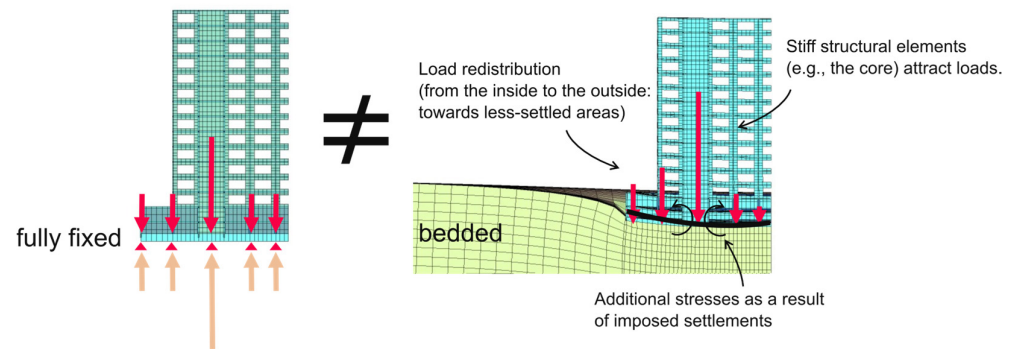


**Figure 1.** Conceptual illustration of settlement-induced load redistribution. **Left:** Structure on a fully fixed foundation with uniform support. **Right:** Structure on deformable soil (bedded), showing additional loads and redistribution from inner to outer elements due to imposed settlements.

As mentioned in these sources, the key factor influencing the relevance of variable loads for settlement is their duration of action relative to the time-dependent deformation behavior of the soil. In [9] this behavior is investigated related to the suggested load combinations. In drained, coarse-grained soils (e.g., sands or gravels), loads act directly as effective stresses and result in immediate deformation. In such cases, a larger share of the variable load can be assumed to contribute to settlement (Figure 2a).

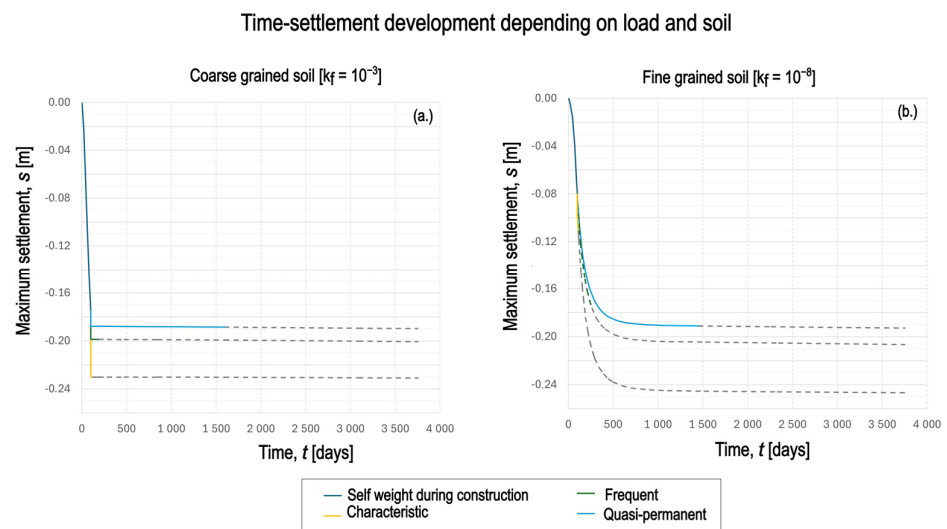


**Figure 2.** Settlement development over time for different load combinations in (a) coarse-grained soil ( $k_f = 10^{-3}$ ) and (b) fine-grained soil ( $k_f = 10^{-8}$ ). The curves compare settlements under self-weight during construction, characteristic, frequent, and quasi-permanent load combinations.

In contrast, undrained or time-dependent fine-grained soils (e.g., silts or clays) exhibit delayed deformation mechanisms such as consolidation and creep. In these materials,

loads only develop significant settlement-relevant stresses after sufficient time has passed. Short-term actions are therefore generally negligible in the context of long-term settlement—except for the immediate undrained initial deformation (Figure 2b).

To assume the overall settlement behavior in fine grained soils with low permeability right, a proper assumption of the permanent live loads must be performed. Live load Measurements of [10] show some deviations compared to its quasi permanent proportion within the Eurocode [11] and are given in Figure 3.

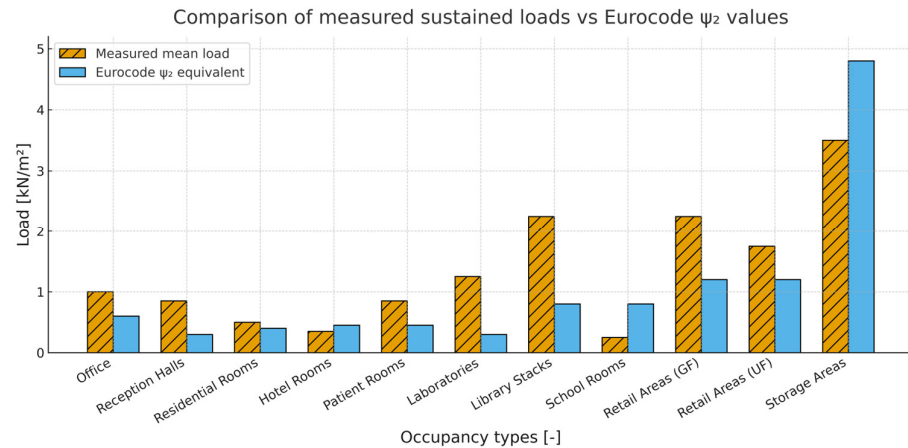


**Figure 3.** Comparison of measured mean sustained live loads from various occupancy types with corresponding Eurocode Quasi-permanent values.

Considering cultural and regional differences, several studies from different countries—including [12–16]—provide extensive data on sustained live loads in office buildings. Variations between results can be attributed to cultural practices, office usage, equipment, survey methodology, time intervals, and sample sizes. Reported mean values range between  $0.31 \text{ kN/m}^2$  and  $0.83 \text{ kN/m}^2$ , with an average standard deviation of about  $0.40 \text{ kN/m}^2$ . A trend towards lower sustained loads with increasing floor area is evident. Peaks such as the  $2.05 \text{ kN/m}^2$  measured in a storage room are rare and highly localized. This study is discussed in detail in [17]. As illustrated in Figure 4, measured sustained loads are generally lower than the Eurocode  $\psi_2$ -based design value, which may be considered in settlement-relevant load combinations and can be assumed as the lower boundary condition for loading.

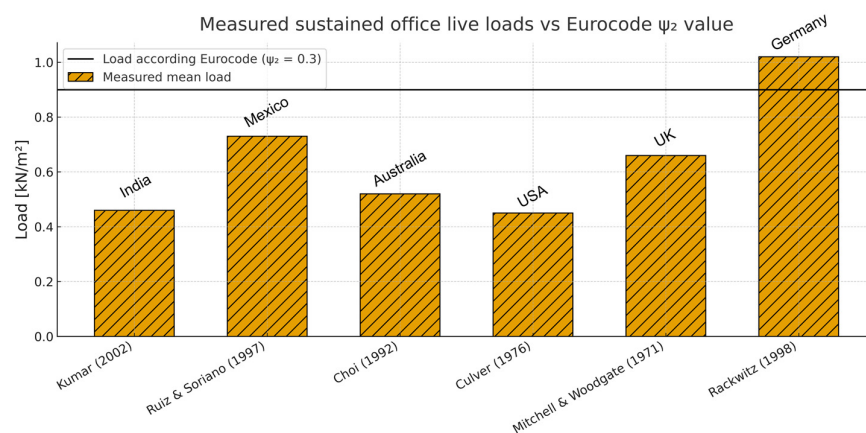


**Figure 4.** Measured sustained live loads in offices from different studies and countries compared to the suggested quasi-permanent load according to Eurocode: India [12], Mexico [13], Australia [14], USA [15], UK [16] and Germany [10].

The upper bound of the settlement-relevant load range is defined by the characteristic combination of live loads. Stochastic simulations of live loads in [18,19] demonstrate that the characteristic values prescribed in Eurocode EN 1991-1-1 [20] and national annexes are generally conservative, especially for office buildings, and applies relatively high  $\alpha$ -reduction factors, particularly for multiple floors, resulting in limited load reduction. In contrast, the UK National Annex [21] permits significantly lower  $\alpha$ -values, allowing more substantial reductions with increasing number of floors, while the French annex [22] adopts intermediate values, considering differences between office- and residential buildings. These differences, shown in Figure 5, highlight the potential for a more differentiated and less conservative approaches, aligning better with probabilistic results without compromising safety and may be an acceptable assumption for drained coarse-grained soils.

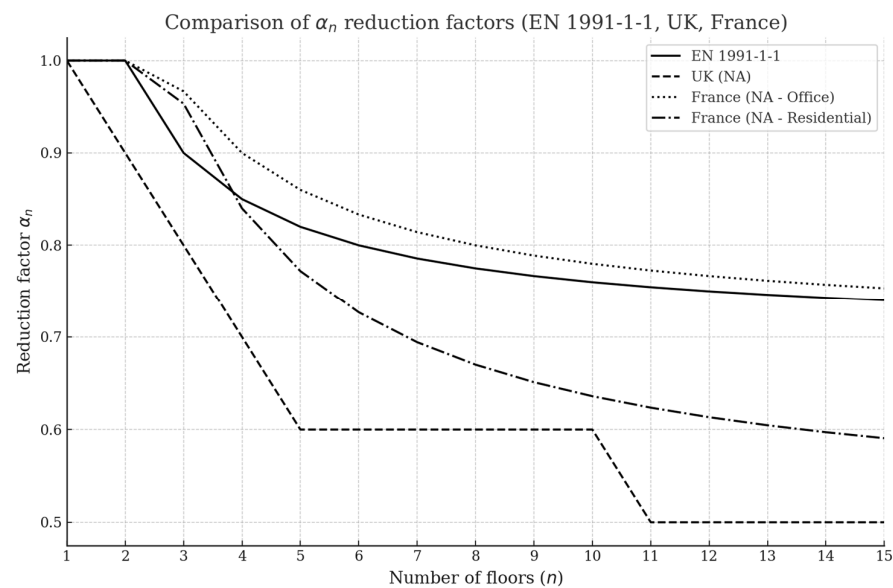


**Figure 5.** Comparison of  $\alpha_n$  reduction factors according to EN 1991-1-1 and the National Annexes of the UK and France.

## 2. Materials and Methods

The structural model applied in this study has been extensively verified and published in previous works [23]. The coupled geotechnical–structural FE model was benchmarked against this reference model [24] for comparable linear soil conditions, resulting in settlement deviations of approximately 1%, confirming its reliability for the present investigation. While no direct validation against large-scale experimental or field data was possible due to the lack of suitable datasets, field measurements from [25] are referenced as a potential benchmark for future studies.

To evaluate the influence of structural stiffness and different building types on the load redistribution behavior two contrasting construction types are analyzed:

- A relatively flexible frame-type system,
- A relatively stiff wall-type system.

All relevant material parameters, cross-sectional dimensions, and geometric building dimensions are summarized in Table 1 and illustrated in Figure 6. These serve as the basis for the subsequent parametric analysis. The structural models and the resulting load distributions used in the geotechnical simulations were developed using the SOFiSTiK (Version 2023) structural analysis software [26].

**Table 1.** Overview table for thickness of structural components and material properties.

Structural Component	Thickness	Material Property	Value
Foundation slab [m]	1.75	Poisson's ratio $\nu$ [-]	0.2
Floor slab [m]	0.28	Elastic modulus E [MPa]	30,000
Columns [m]	0.50	Concrete unit weight [kN/m <sup>3</sup> ]	25
Exterior & interior walls [m]	0.20	Flooring load [kN/m <sup>2</sup> ]	2
Basement & core walls [m]	0.30	Facade load [kN/m <sup>2</sup> ]	3.5

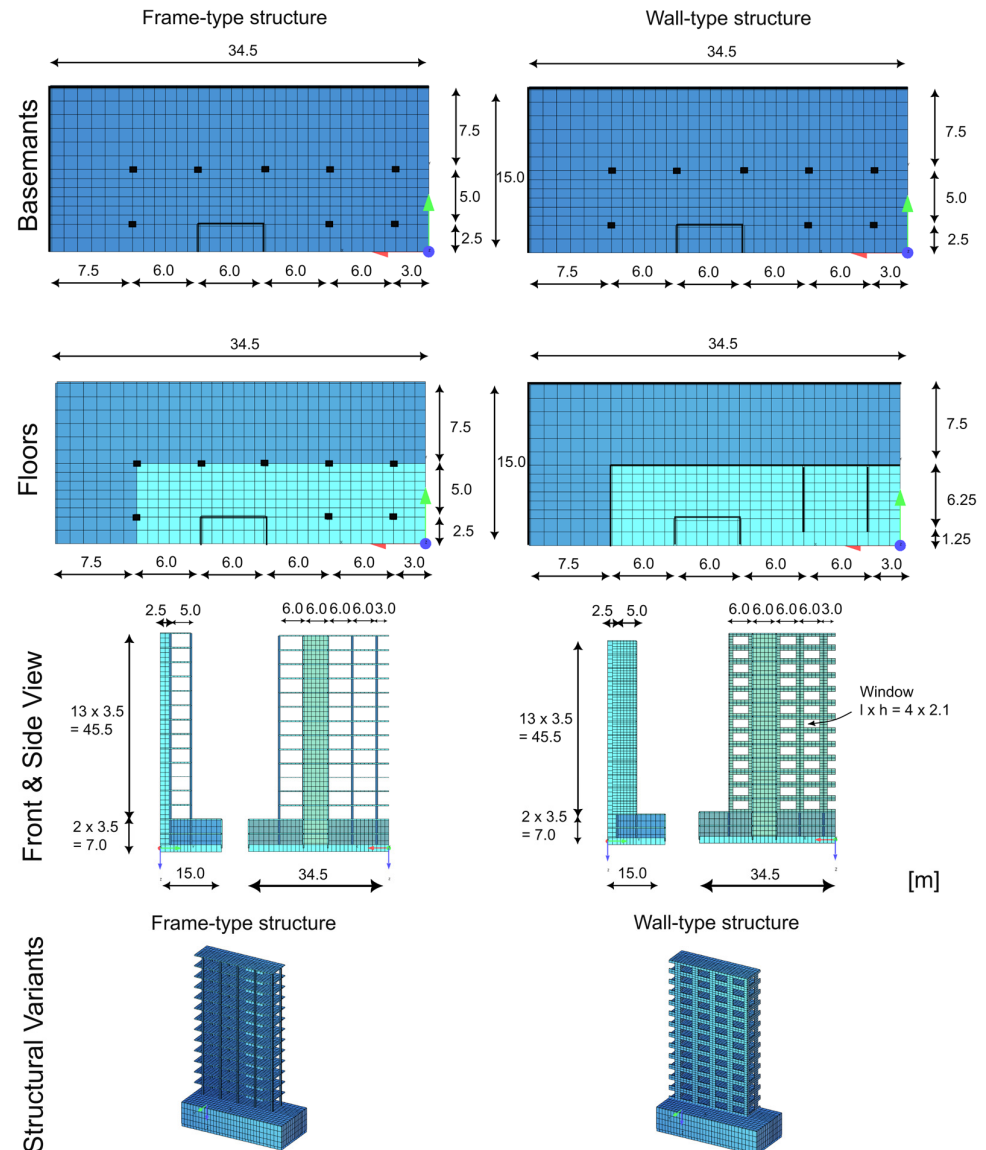


**Figure 6.** Overview of the selected model variants for analyzing superstructure stiffness influence. The figure contrasts frame-type and wall-type configurations, each with either small or large basements. The intermediate rows show floor layouts and elevation views. The bottom row illustrates the combined 3D models. These models serve as the basis for evaluating differential settlements under varying soil conditions and structural configurations.

The geotechnical analyses are conducted using numerical simulations in PLAXIS 3D [27]. All models are defined as doubly symmetric, reducing computational effort while maintaining physical accuracy (Figure 7). Model boundaries are placed sufficiently far from the area of interest to avoid boundary effects, following the recommended dimensions in [28]. Boundary conditions include:

- Fixed horizontal displacements along the model boundaries and symmetry planes,
- A fully fixed base, and
- No-flow conditions at the bottom and along symmetry planes for consolidation analyses.

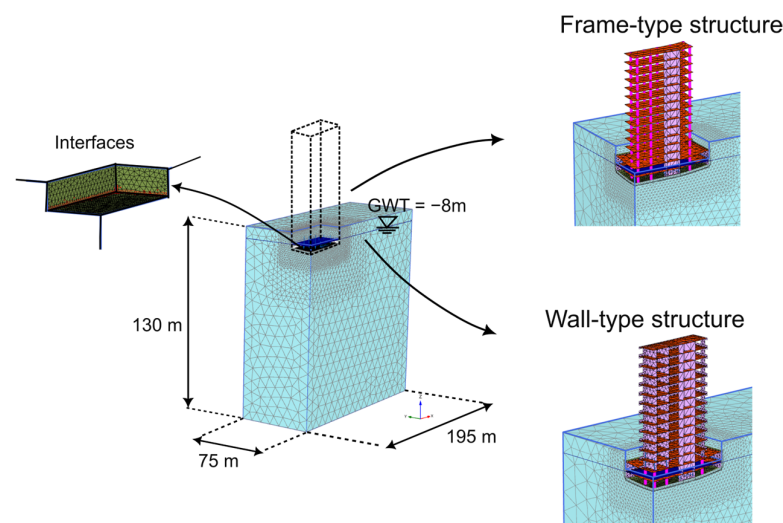


**Figure 7.** Geotechnical model setup and integrated structural variants. The central domain illustrates the 3D soil continuum used in the PLAXIS simulations, including boundary conditions, symmetry planes, and groundwater table at -8 m depth. A zero-thickness interface is defined at the contact between foundation, the cellar walls and soil. The model contains approximately 46,000 soil elements using 10-node tetrahedra elements.

The construction sequence is modeled as follows:

- **Initial phase:** Generation of initial in situ soil stresses.
- **Excavation phase:** Deactivation of the building pit; pit walls supported by prescribed displacements, which are fixed to zero; reset small-strain and displacements to zero.
- **Foundation phase:** Activation of the foundation slab including self-weight; reset displacements to zero.
- **Superstructure phase:** Activation of the “as-built” structure represented by linear-elastic plate and beam elements; surface loads corresponding to the selected load combinations applied; reset displacements to zero.
- **Consolidation analysis (optional):** Time-dependent analysis over a period of 30 years.
- **Sequenced loading (optional):** Final increase in variable loads after consolidation.

Both drained and undrained conditions are investigated, including time-dependent consolidation behavior. At the contact between the basement wall and the surrounding soil, a zero-thickness interface is defined. To realistically represent shear transfer, an interface reduction factor of  $R_{inter} = 0.9$  at the bottom and 0.85 at the cellar walls is applied based on the studies made in [29].

The soil domain is discretized using 10-node tetrahedral elements, and advanced nonlinear constitutive soil models are employed. The superstructure is modeled using elastic plate and beam elements, representing the structural stiffness in a mechanically consistent but simplified way.

Extensive validation analyses were carried out by comparing results from the original SOFiSTiK structural model with the PLAXIS-based geotechnical reconstruction under identical boundary conditions. The resulting differential settlements differ by less than 1%, confirming that the structural stiffness representation in PLAXIS is sufficiently accurate for the purpose of this study.

To capture a broad range of soil behavior, three representative soil types were selected: clay, silt, and sand. For each soil, a representative Hardening Soil with Small-Strain (HSS) parameter set was defined (Table 2). The selected soil types and structural configurations are intended to serve as representative reference points rather than exact real-case scenarios. A full sensitivity analysis of soil parameters was not performed, as the objective of this study is to provide a theoretical basis for understanding settlement-induced force redistribution. For practical applications, parameter sensitivity should be assessed for each specific soil–structure configuration.

**Table 2.** Overview table of the selected soil types. General soil parameters based on [30] and modified for HSS application using [31]. HSS model parameters:  $\gamma_u$  = unsaturated unit weight,  $\gamma_{sat}$  = saturated unit weight,  $k_f$  = permeability,  $\varphi'$  = friction angle,  $c'$  = cohesion,  $\psi'$  = dilatancy,  $\nu_{ur}$  = Poisson's ratio,  $E_{oed}^{ref}$  = oedometric modulus,  $E_{50}^{ref}$  = secant module,  $E_{ur}^{ref}$  = unloading/reloading module,  $m$  = stiffness exponent,  $G_0^{ref}$  = shear modulus for small deformations,  $\gamma_{0.7}$  = limit for small shear strains,  $K_0^{NC}$  = horizontal earth pressure coefficient for normally consolidated soil,  $p^{ref}$  = reference pressure for all stiffness parameters 100 kN/m<sup>2</sup>.

Soiltype	$\gamma_u$ [kN/m <sup>3</sup> ]	$\gamma_{sat}$ [kN/m <sup>3</sup> ]	$k_f$ [m/s]	$\varphi'$ [°]	$c'$ [kN/m <sup>2</sup> ]	$\psi'$ [°]	$\nu_{ur}$ [-]	$E_{oed}^{ref}$ [kN/m <sup>2</sup> ]	$E_{50}^{ref}$ [kN/m <sup>2</sup> ]	$E_{ur}^{ref}$ [kN/m <sup>2</sup> ]	$m$ [-]	$G_0^{ref}$ [kN/m <sup>2</sup> ]	$\gamma_{0.7}$ [-]	$K_0^{NC}$ [-]
Clay	20.5	21	10 <sup>-10</sup>	28	2	0	0.2	4000	7000	30,000	1.0	50,000	$2 \times 10^{-4}$	0.53
Silt	19.0	20	10 <sup>-8</sup>	29	2	0	0.2	12,000	16,000	47,000	0.7	78,300	$1 \times 10^{-4}$	0.51
Sand	17.5	20	10 <sup>-4</sup>	36	0	6	0.2	30,000	30,000	90,000	0.5	150,000	$1 \times 10^{-4}$	0.41

This study focuses on the sustained part of variable loads because their magnitude and duration are decisive for settlement behavior. Settlement analysis was carried out considering the relevant actions over the governing time period as required by EN 1997 [32], with the classification of permanent, variable, and accidental actions taken from EN 1990 [1]. Short-term actions such as wind, earthquakes, and accidental loads were excluded as they are not decisive for settlement behavior.

To assess the influence of different load combinations on load redistribution and their relevance in structural design, Table 3 summarizes the variable live loads considered. The example refers to Category B2—Offices according to EN 1991-1, with a characteristic load  $q_c = 4.2$  kN/m and  $n = 15$  floors. The reductions according to  $\alpha_n$  and the application of  $\psi$ -factors for frequent and quasi-permanent combinations are shown. While  $\alpha_n$ -values vary internationally (e.g., 0.75 in EN vs. 0.5 in UK/French Annexes), only the EN values were analyzed here, as the objective is to demonstrate the general effect of reducing sustained variable loads rather than to compare specific national regulations. The identified findings and trends can thus be applied in relation to the proportion of sustained variable loads and are transferable to other load combination systems.

**Table 3.** Variable load depending on load combination and number of floors ( $n = 15$ ).

Load Combination	Formula	Result
Characteristic	$q_C = q = 4.2$	$q_C = 4.2$ kN/m <sup>2</sup>
Characteristic reduced by $\alpha_n$	$q_\alpha = q \cdot \alpha_n = 4.2 \left(0.7 + \frac{0.6}{n}\right)$	$q_\alpha = 3.1$ kN/m <sup>2</sup>
Frequent	$q_F = q \cdot \psi_1 = 4.2 \cdot 0.5$	$q_F = 2.1$ kN/m <sup>2</sup>
Quasi-permanent	$q_{Q-p} = q \cdot \psi_2 = 4.2 \cdot 0.3$	$q_{Q-p} = 1.3$ kN/m <sup>2</sup>

To ensure a comprehensive and consistent comparison between the structural models, several key parameters are evaluated. As illustrated in Figure 8, these include the normal

forces in the outer and inner columns as well as in the core, providing insight into how force redistribution occurs within the structure. In addition, the maximum bending moment beneath the core and the field moment in the middle span are monitored to identify any relevant changes in the fundamental design forces of the foundation slab. Finally, the overall settlement behavior is assessed, including the maximum settlement at the center of the structure and the minimum settlement at the outer corner, to determine whether the structural response remains within realistic limits.

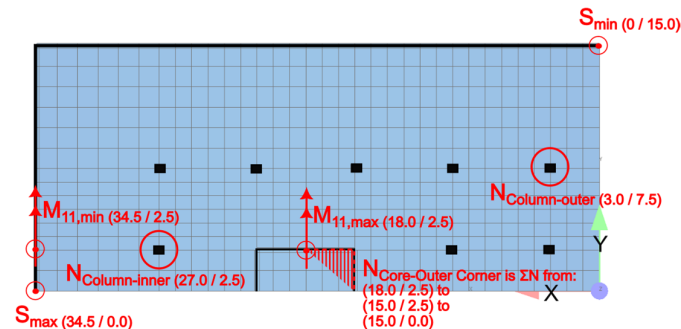


**Figure 8.** Overview of evaluation parameters for comparison of structural models. Monitored values include normal forces in outer and inner columns and the core, maximum bending moment beneath the core, field moment at midspan, and settlements (maximum at center, minimum at outer corner).

This study employs a deterministic approach focusing on selected case studies to provide an initial understanding of settlement-induced force redistribution. The results should be interpreted as indicative trends rather than general design rules, as several aspects are beyond the current scope:

- **Methodological constraints:**
  - Deterministic modeling without a full probabilistic framework.
  - No validation against large-scale experimental data due to lack of suitable datasets.
  - Use of the HSS model only, without comparison to other advanced constitutive models.
- **Structural limitations:**
  - Only two idealized, symmetric structural systems (flexible frame-type and stiff wall-type).
  - No consideration of asymmetric layouts, eccentric loading, or adjacent structures.
  - Linear-elastic modeling of the foundation slab, without cracking or concrete creep.
- **Geotechnical simplifications:**
  - Primary consolidation only, without soil creep.
  - No anisotropy in stiffness or permeability.
  - Fixed groundwater table, neglecting seasonal fluctuations.
  - No coupled thermal–hydro–mechanical effects.

These simplifications were made to isolate the fundamental mechanisms of settlement-induced force redistribution. The two systems investigated were deliberately chosen as representative extremes to illustrate the influence of structural stiffness. Future work will address parameter variability, foundation types, and enhanced soil models as part of a broader research program aimed at developing practical guidelines for soil–structure interaction.



Generative AI has been used in this study primarily for linguistic refinement of the drafted text. Literature searches were supported by AI-based keyword and topic suggestions, but all identified sources were manually reviewed and evaluated by the authors. Preliminary sketches generated by AI tools were digitally converted and subsequently visually inspected and finalized by the authors.

### 3. Settlement Relevant Load Combination

#### 3.1. Load Redistribution Depending on Load Combination

A common and recommended approach for considering the influence of settlements on structural behavior is to first determine the settlement distribution using a geotechnical program capable of capturing the complex, nonlinear behavior of soil. The resulting settlements can then be imposed on the structural foundation elements within the structural model. This prescribed deformation leads to a redistribution of internal forces within the structure, typically from areas with larger settlements (often the center) toward less affected zones (usually the edges). As these imposed settlement troughs are constant under an applied load (unlike those derived from linear-elastic soil approximations or subgrade reaction modules used in structural programs), it must be ensured that the resulting restraining effects are representative and sufficiently safe for the range of load variations encountered in structural design.

In this study, the restraining effects are evaluated by comparing the axial forces of the settlement model to a reference model without settlements. The reference normal force is obtained from a fully fixed support condition and defined as

$$N_{\text{reference}} = N_{(\text{fixde support, no settlements})} = 100\%. \quad (1)$$

The restraining ratio is then given as the relative axial force in the settlement case with respect to this reference:

$$\rho_{\text{restr}} = \frac{N_{\text{with settlement}}}{N_{\text{reference}}} 100 [\%]. \quad (2)$$

Values of  $\rho_{\text{restr}} > 100\%$  indicate a relief of forces (e.g., in inner columns), while  $\rho_{\text{restr}} < 100\%$  correspond to additional loading (e.g., in outer columns or core edges). In the diagrams, the reference force is always plotted as 100%. The gray bars show the axial forces obtained from the settlement model, while the hatched sections illustrate the deviation from the reference, which is attributed to restraining effects. This concept follows the general definition of restraint effects as introduced in EN 1992-1-1 [33] and fib Model Code 2010 [34].

This study therefore investigates how the restraining ratio evolves depending on the applied load combination and identifies which combination should be considered settlement-relevant for deriving a representative settlement trough for structural design. The settlement distributions resulting from these combinations are evaluated based on their impact on internal force redistribution, focusing on selected structural elements and extracted directly from the PLAXIS 3D model. This eliminates the need for data exchange with a separate structural program and ensures full consistency between soil response, foundation behavior, and the resulting internal force redistribution.

To this end, four different load combinations are applied, each representing a plausible range of loading as defined in Eurocode:

- the quasi-permanent combination,
- the frequent combination,
- the characteristic combination with partial reduction factor  $\alpha_a$ ,
- the characteristic combination.

To explore the influence of structural stiffness on load redistribution, two representative building types are analyzed: a comparatively stiff wall-type structure and a more flexible frame-type structure. Each building is placed on three different soil types—sand, silt, and clay—under drained conditions. In this study, silt and clay are included as representatives of soft, low-stiffness soils, while sand represents stiffer soil conditions. Permeability effects and time-dependent behavior are intentionally neglected to focus on the influence of soil stiffness on settlement-induced force redistribution. This allows for a comparison of how soil type and stiffness influence the load redistribution triggered by settlements.

For each case, the selected load combination is first applied to a model with fully fixed supports to establish a reference load distribution. Subsequently, the same combination is used in the geotechnical model to simulate the resulting settlements and analyze their impact on structural behavior.

Figure 9 presents the total normal force acting on three representative structural members—the inner column, outer column, and the outer core edge—under various load combinations and soil conditions.

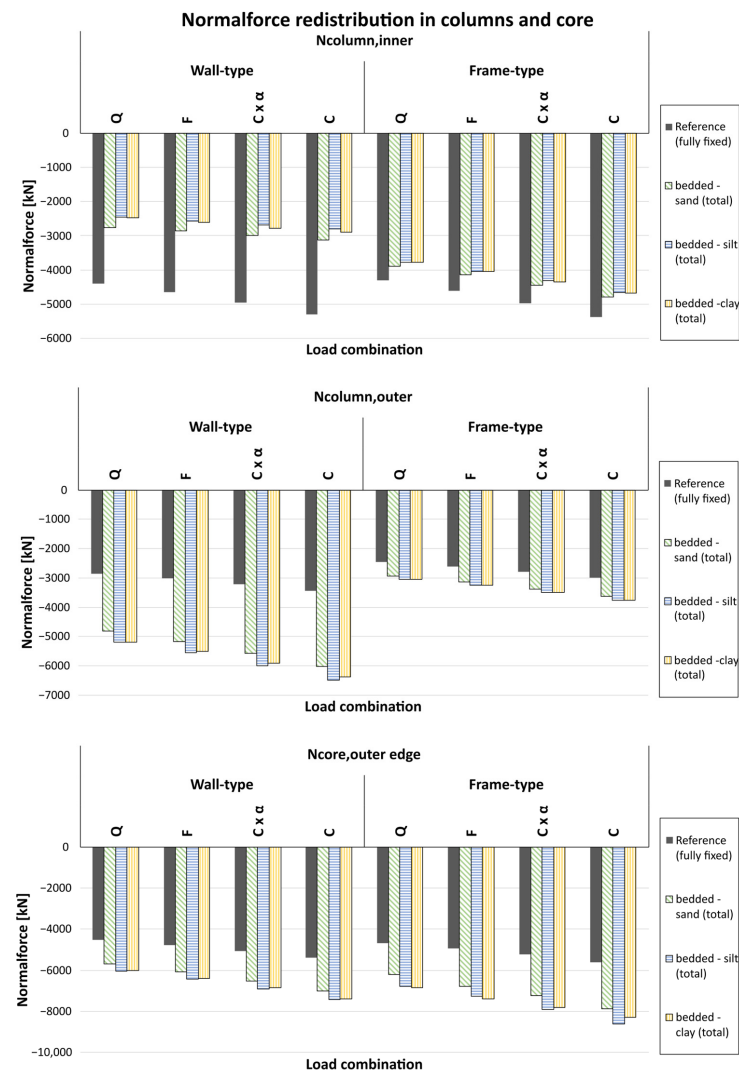


**Figure 9.** Total normal force in selected structural members (inner column, outer column, outer core edge) under various load combinations and soil types for a Wall-type and Frame-type structure. The gray bars represent the reference case with fully fixed supports (no settlements). Colored bars show results for different bedding conditions (sand, silt, clay).

The grey bars represent the reference case, calculated using a fully fixed model without soil–structure interaction. As expected, the normal force in these members increases with the load level, reflecting the unaltered internal force distribution.

When bedding is considered, however, the results show a clear redistribution of internal forces caused by differential settlements. In general, loads are redistributed from the inner column, located in the more heavily settled central area, toward the outer column and the core edge, which are less affected by settlement and typically stiffer. This redistribution pattern is especially pronounced in the stiffer wall-type structure, where differential settlements induce stronger internal force shifts.

Regarding soil type, the redistribution becomes more significant in softer soils, particularly in silt and clay. The greater deformability of these soils leads to increased differential settlements, thereby amplifying the structural response.

An additional observation from the figure is that stiff elements, such as the core edge in the frame-type structure, attract a disproportionately high share of restraining forces. This indicates that in flexible structures, local stiffness variations (e.g., stiff core vs. flexible frame) enhance the settlement-induced redistribution more strongly than in generally stiff systems.

In all members, the total normal force increases with higher load combinations. However, the relative contribution of restraining forces behaves differently depending on structural stiffness, soil type, and member location as shown in Figure 10.

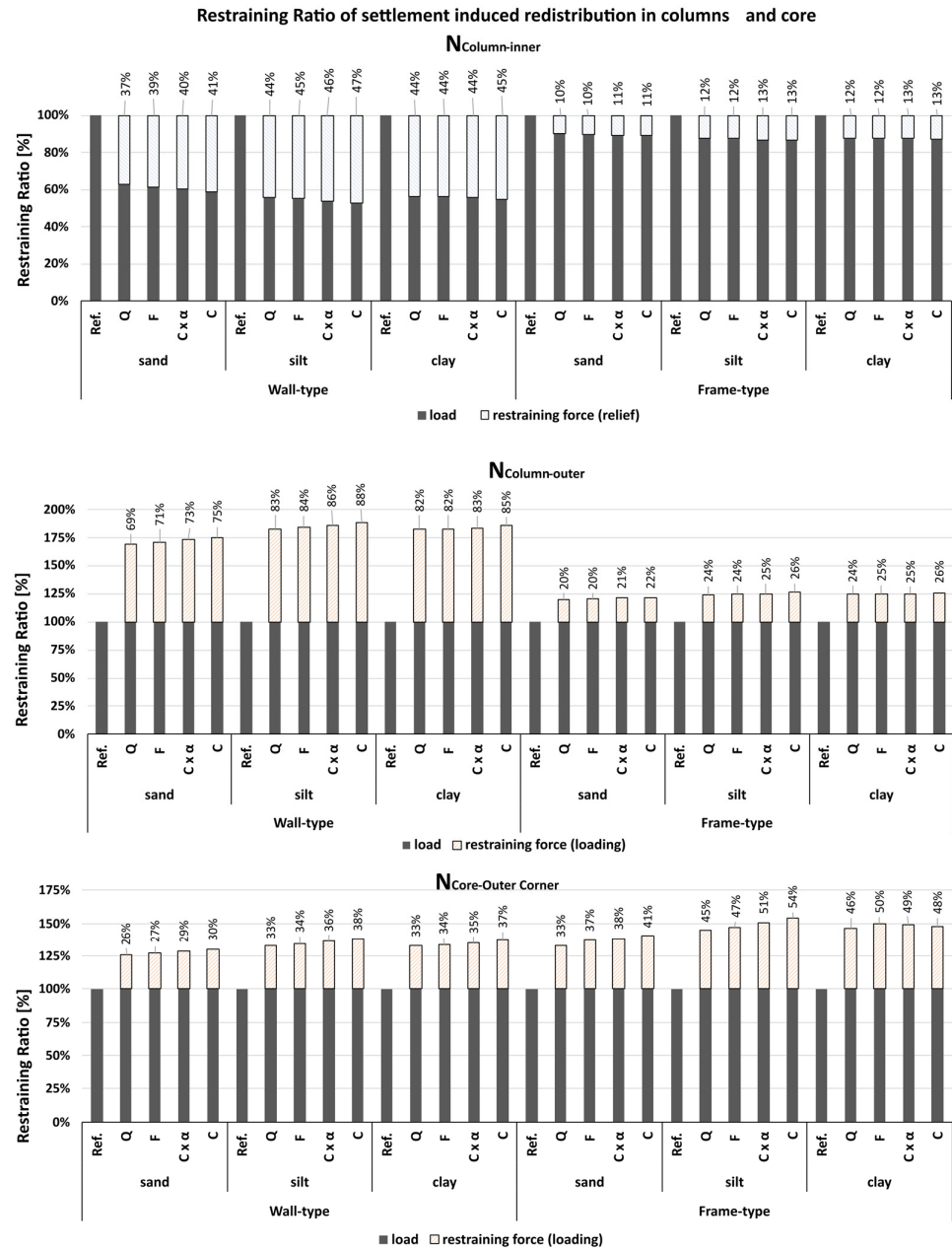
For the inner column, a significant share of the total force is relieved due to settlement-induced redistribution in the wall-type structure, ranging between 37% and 45%, depending on the load combination and subsoil. In contrast, the frame-type structure, being more flexible, shows a much lower restraining effect—only 10% to 13% of the total force is relieved due to settlement-induced restraint.

Across all soil types, the variation in restraining ratio due to load combination is relatively small. For the wall-type on sand, the restraining share increases from 37% (quasi-permanent) to 41% (characteristic), a difference of 4%. In silt, this range narrows to 3%, and in clay, to just 1%, indicating that with softer soils, the relative effect of load level on restraint becomes less pronounced.

In the outer column, the restraining component is positive, reflecting additional loading due to the outward redistribution of forces. The wall-type structure again exhibits stronger restraint, with restraining shares from 69% to 88%, whereas the frame-type structure shows a much smaller increase of only 20% to 26%. Also here, the influence of load combination decreases with softer soils: for the wall-type on sand, the restraining force increases by 6% across load combinations, while in clay, the difference drops to 3%. For the frame-type, the total variation remains around 2%, confirming the lower sensitivity of flexible systems.

The core's outer edge shows high restraining effects in both structural types. Interestingly, the restraining share is even higher in the flexible frame-type structure, with values ranging from 33% to 54%, compared to 26% to 38% in the stiffer wall-type structure. This suggests that local stiffness—even within a globally flexible system—can attract significant restraining forces when differential settlements occur.

Moreover, the range of restraining variation across load combinations is largest in the core region. While the wall-type shows a moderate variation of about 4%, the frame-type exhibits higher sensitivity (8%), especially on clay, where the restraining share increases from 46% (quasi-permanent) to 50% (frequent) and slightly decreases to 48% (characteristic). This could potentially be explained by plastic deformation effects in the outer clay regions, which may reduce differential settlements locally and balance loads at higher load levels. An effect already discussed in former works [35].



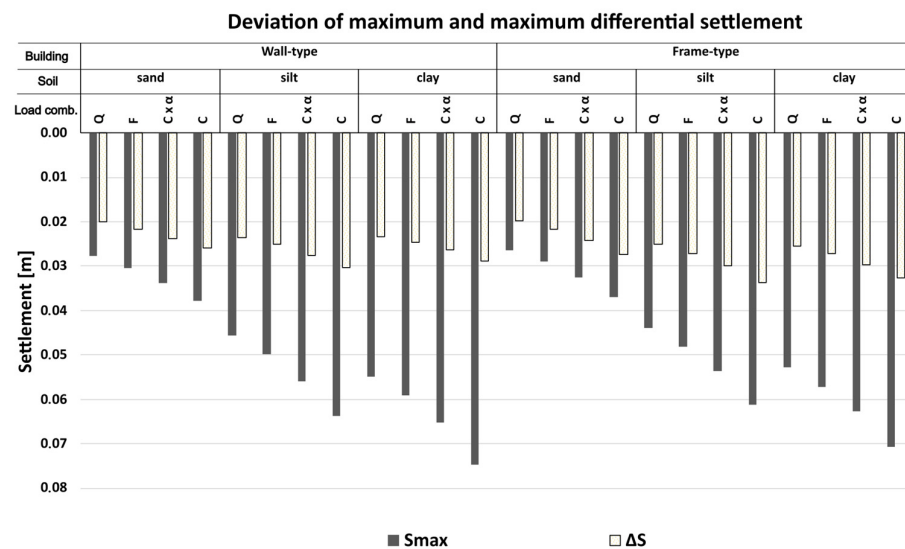
**Figure 10.** Settlement-induced restraining forces in key structural members under various load combinations and soil conditions. Gray bars show the normalized load-induced normal force; hatched bars indicate the additional restraining component from settlements. Restraint reduces forces in the inner column (**top**) but increases them in the outer column (**middle**) and core corner (**bottom**).

Figure 10 illustrates the comparison of maximum and differential settlements under various load combinations, normalized with respect to the characteristic load combination. The gray bars represent the maximum settlement  $S_{max}$ , while the yellow bars show the maximum differential settlement ( $\Delta S$ ). Both are expressed as a percentage of the values resulting from the characteristic load combination (defined as 100%).

The results indicate a substantial reduction in settlement when the quasi-permanent load combination is applied. For maximum settlements, the quasi-permanent load case on sand leads to values of approximately 73% in the wall-type structure and 71% in the frame-type structure, compared to the characteristic case. This behavior is consistent across all soil types.

A similar trend is observed for differential settlements. The quasi-permanent combination results in about 77% of the characteristic  $\Delta S$  in the wall-type structure and 73% in the frame-type structure. These findings emphasize that load level has a major impact not only on absolute but also on relative (differential) settlements. Notably, this effect appears largely independent of structural stiffness and soil type, suggesting that the choice of load combination has a dominant influence on settlement magnitudes in general.

Figure 11 shows the influence of settlements—particularly differential settlements—on the distribution of bending moments within the foundation slab. As expected, the variation in maximum and minimum bending moments correlates with the behavior observed in the previous figure on settlements, indicating a direct link between soil-induced deformations and internal structural forces.



**Figure 11.** Normalized maximum settlement ( $S_{max}$ ) and differential settlement ( $\Delta S$ ) for various load combinations, soil types, and structural systems.

Figure 12 now shows how the maximum bending moments ( $M_{11,max}$ ) in the core region consistently follow the increasing load level. For both structural types, values start at around 80% (relative to the characteristic load combination) under quasi-permanent loading and increase proportionally with the applied load combination, independent of soil type. This confirms that bending moment magnitudes are primarily governed by the load level and are less sensitive to soil stiffness in this context.

The minimum bending moments ( $M_{11,min}$ ) observed in the slab field, however, show more variation—both between structural types and across soil conditions. For example, in sand, the wall-type structure reaches 70% of the characteristic moment under quasi-permanent loading, whereas the more flexible frame-type structure shows only 59%. For the frame-type structure, a clear trend with soil stiffness is visible: 59% in sand, 67% in silt, and 73% in clay.

This indicates that foundation elements of flexible structures react more sensitively to differential settlements, especially in stiffer soils, where the moment distribution shows larger relative deviations from the characteristic loading case.

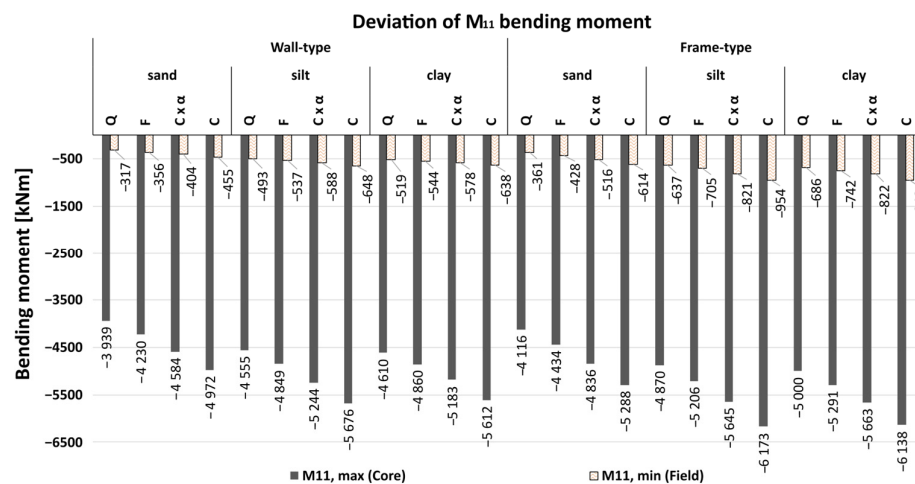


**Figure 12.** Normalized maximum and minimum bending moments ( $M_{11}$ ) in the foundation slab under different load combinations, soil types, and structural systems. The dark gray bars show the maximum bending moment in the core region, while the orange bars represent the minimum moment in the slab field. Moments are evaluated consistently at the same gauss point closest to the investigated location (see Figure 7). As the study focuses on relative differences between load combinations, this approach ensures consistency, and minor deviations in absolute values are negligible.

### 3.2. Influence of Permeability on Settlement Relevant Load Combination

As outlined in the introduction, for soils with low permeability and groundwater presence, a sustained load over a certain duration is required to generate volumetric deformation and settlement. Rapid load changes or short-term peaks, as represented by frequent or characteristic load combinations in structural design, are generally insufficient to induce significant consolidation settlements. Instead, they mainly cause volume-constant shear deformations typically for undrained behavior. Accordingly, the quasi-permanent load combination is typically recommended as the basis for long-term settlement analysis in such soils.

The objective of this analysis is to determine whether a sequenced loading case—representing a sudden short-term load increase after long-term consolidation—produces a settlement distribution that could be decisive for structural design. We hypothesize that, despite altering internal stresses, such a short-term load does not generate a new, critical settlement shape compared to the long-term consolidated state.

To investigate this, a case study was conducted on the wall-type building, comparing:

1. **Time-consolidated settlement case:** Continuous quasi-permanent loading over 30 years, representing the long-term settlement trough in cohesive soils.
2. **Sequenced loading case:** A sudden application of the reduced characteristic load combination (including  $\alpha$ ) for one day after 30 years of consolidation.

This comparison evaluates whether short-term load variations can create a new, governing settlement distribution for design purposes.

Figure 13 shows that when considering time-dependent settlement behavior, the restraining effect in structural elements increases. For silt, the transition from quasi-permanent drained to quasi-permanent consolidated loading leads to an increase of approximately 2% in both the inner and outer columns and around 1% in the core.

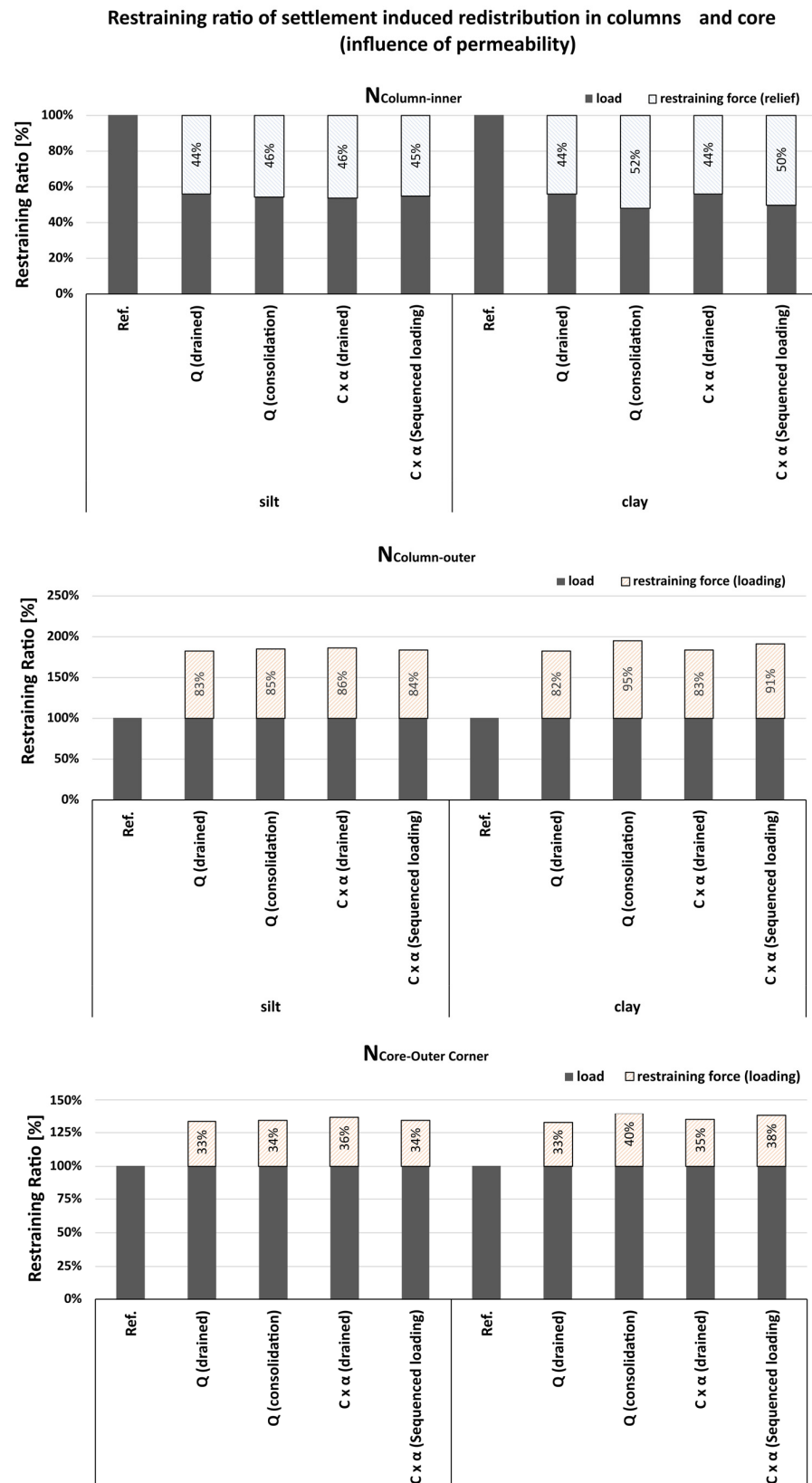


**Figure 13.** Relative load and restraining force components in selected structural elements (inner column, outer column, core outer corner) under various loading scenarios and soil conditions. The figure compares results for drained quasi-permanent loading, long-term consolidation, and sequenced loading (short-term application of reduced characteristic load after consolidation) on silt and clay. Gray bars represent the load-induced portion; hatched areas indicate the restraining component—acting as load relief (blue) or additional loading (red).

In contrast, for clay, which exhibits much lower permeability and stronger time-dependent behavior, the restraining effect increases significantly. The inner column shows an increase of 8%, the outer column of 13%, and the core of 7%, clearly emphasizing the relevance of soil permeability and consolidation effects in long-term settlement analysis.

Looking now at the sequenced loading case—where after long-term consolidation under quasi-permanent loading, a short-term application of the reduced characteristic load is superimposed—it becomes apparent that this temporary loading spike does not increase the restraining effect. Instead, a slight reduction in restraining forces can be observed. This is likely due to additional plastic deformations occurring under undrained conditions, which locally reduce stiffness and thus limit further redistribution.

From a structural design perspective, it would only be necessary to consider such a short-term settlement distribution—instead of the long-term quasi-permanent case—if the resulting internal force redistributions exceeded the range observed under realistic service conditions. However, this is not the case in the present study. The additional effects of sequenced loading remain within the expected variation and do not justify separate consideration in settlement-relevant design procedures.

Regarding the bending moments, Figure 14 shows that the **sequenced load combination** results in approximately a 10% higher maximum bending moment in the foundation slab and a 9% higher field moment in silt. In nearly impermeable clay, this difference decreases to about 8% for the maximum moment and 5% for the field moment.

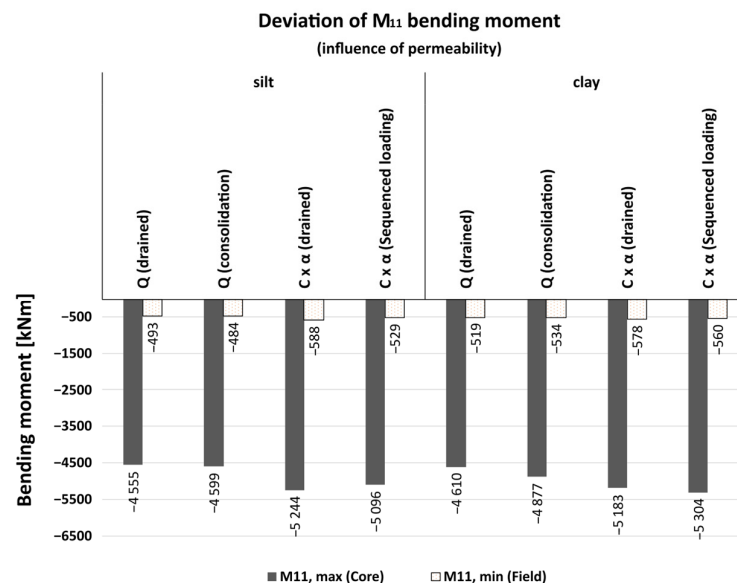


**Figure 14.** Bending moments  $M_{11}$  in the foundation slab for different load combinations and soil types (silt and clay) considering time effects. Moments are evaluated consistently at the same Gauss point closest to the investigated location (see Figure 7). As the study focuses on relative differences between load combinations, this approach ensures consistency, and minor deviations in absolute values are negligible.

#### 4. Conclusions

This study indicates that the stiffness of a structure plays an important role in how internal forces are redistributed when settlements occur. In the analyzed cases, stiffer structures tended to show more pronounced redistribution, making it necessary to account for bedding effects in the design process. Soft soils resulted in higher absolute restraining forces, while their sensitivity to different load combinations was less significant. Local stiffness concentrations, such as cores, were particularly affected, especially when embedded in flexible buildings on soft soils.



Within the investigated scenarios, the choice of settlement-relevant load combinations proved critical for deriving representative settlement troughs. The characteristic combination appeared conservative and should be reduced using the floor reduction factor  $\alpha_n$ . The quasi-permanent combination represented a realistic lower limit and should not be reduced further. For drained coarse-grained soils, the reduced characteristic combination (including  $\alpha_n$ ) offered a reasonable balance between safety and realistic deformations. For cohesive soils with low permeability, long-term quasi-permanent loading was more appropriate, as consolidation significantly influenced both settlements and internal forces. Short-term load variations following long-term consolidation did not lead to new decisive settlement shapes and can therefore be considered through safety factors rather than through separate settlement load cases.

While these findings provide useful indications for selecting settlement-relevant load combinations, they are based on a limited number of case studies and idealized assumptions. The results should therefore be understood as indicative trends for the investigated configurations rather than general design rules. Aspects such as nonlinear structural behavior (e.g., cracking and creep in reinforced concrete), anisotropic and time-dependent soil response, asymmetric building layouts, and external influences such as groundwater fluctuations or adjacent structures were not included. Considering these aspects, as well as extending the analyses to a broader range of structural configurations and probabilistic parameter studies, will be an important focus of future research aimed at developing more comprehensive guidelines for soil–structure interaction.

**Author Contributions:** Conceptualization, C.W. and J.R.; investigation, C.W. and J.R.; writing—original draft preparation, C.W.; writing—review and editing, C.W. and D.S.; supervision, D.S.; All authors have read and agreed to the published version of the manuscript.

**Funding:** This work was supported by the Open Access Fund of Graz University of Technology.

**Data Availability Statement:** The data presented in this study are available on request from the corresponding author.

**Acknowledgments:** This study was conducted within the framework of the collective research project Agile Structural Design for Resource-Responsible Construction, funded by the Austrian Research Promotion Agency (FFG) under project number FO999913808.

**Conflicts of Interest:** Author Jakob Resch was employed by the company IKK Group. The remaining authors declare that the research was conducted in the absence of any commercial or financial relationships that could be construed as a potential conflict of interest.

## References

1. EN1990:2002; CEN Eurocode—Basis of Structural Design. European Committee for Standardization: Brussels, Belgium, 2002.
2. Witt, K.J. *Grundbau-Taschenbuch, Part 3: Foundations and Geotechnical Structures*, 8th ed.; Wilhelm Ernst & Sohn: Berlin, Germany, 2018; ISBN 978-3-433-03153-7.
3. Wendehorst. *Bautechnische Zahlentafeln*, 35th ed.; Springer Vieweg: Wiesbaden, Germany, 2021; ISBN 978-3-658-32792-7.
4. Boley, C.; Schmidt, H.-H.; Buchmaier, R.F. *Handbook of Geotechnics: Fundamentals—Applications—Practical Experience*, 2nd ed.; Springer Vieweg: Wiesbaden, Germany, 2019; ISBN 978-3-658-03054-4.
5. Vogt-Breyer, C.; Schmidt, H.-H.; Buchmaier, R.F. *Fundamentals of Geotechnics*; Springer Vieweg: Wiesbaden, Germany, 2014.
6. Krapfenbauer, T.J. *Construction Tables: Textbook and Handbook for Civil Engineering*, 19th ed.; Austrian Standards Institute: Vienna, Austria, 2013; ISBN 978-3-7100-2872-4.
7. Schlicke, D.; Tschuchnigg, F.; Fischnaller, H.; Pfaff, K. Structural analysis and design of buildings using 3D global models. In *BetonKalender 2024*; Ch. VIII; Ernst & Sohn: Berlin, Germany, 2023; pp. 505–571.
8. Fischer, D. Interaction between soil and structure—Permissible differential settlements and stresses of structures and foundations. In *Mitteilungen des Instituts für Bodenmechanik und Felsmechanik der Universität Karlsruhe*; Heft 21: Karlsruhe, Germany, 2009.
9. Resch, J. Concept for Settlement-Relevant Load Combinations Considering Construction Stages and Soil–Structure Interaction. Master’s Thesis, Institute of Concrete Structures, Graz University of Technology, Graz, Austria, 2025.

10. Rackwitz, R. Actions on structures. In *Der Ingenieurbau; Structural Reliability, Actions*; Ernst & Sohn: Berlin, Germany, 1998; Volume 8, pp. 73–408.
11. *EN 1990:2013; Eurocode—Basis of Structural Design*. Austrian Standards Institute: Vienna, Austria, 2013.
12. Kumar, S. Live loads in office buildings: Point-in-time load intensity. *Build. Environ.* **2002**, *37*, 79–89. [[CrossRef](#)]
13. Ruiz, S.E.; Soriano, A. Design live loads for office buildings in Mexico and the United States. *J. Struct. Eng.* **1997**, *123*, 816–822. [[CrossRef](#)]
14. Choi, E.C.C. Live load in office buildings: Point-in-time load intensity of rooms. *Proc. ICE—Struct. Build.* **1992**, *94*, 299–306. [[CrossRef](#)]
15. Culver, C.G. *Survey Results for Fire Loads and Live Loads in Office Buildings*; National Bureau of Standards Report; National Bureau of Standards: Washington, DC, USA, 1976.
16. Mitchell, G.R.; Woodgate, R.W. *Floor Loadings in Office Buildings: The Results of a Survey*; Building Research Station: Watford, UK, 1971.
17. Smit, G.; Clayton, C. The behaviour of modern flexible framed structures undergoing differential settlements. In Proceedings of the 5th International Young Geotechnical Engineers’ Conference, Paris, France, 31 August–1 September 2013; IOS Press: Amsterdam, Netherlands, 2013; pp. 285–288.
18. Müller, D.; Tran, N.L.; Graubner, C.-A. Stochastic simulation of imposed loads in buildings. In Proceedings of the 12th International Conference on Applications of Statistics and Probability in Civil Engineering (ICASP12), Vancouver, BC, Canada, 12–15 July 2018.
19. Honfi, D. Serviceability floor loads. *Struct. Saf.* **2014**, *50*, 27–38. [[CrossRef](#)]
20. *EN 1991-1-1:2011; Eurocode 1—Actions on Structures, Part 1-1: Densities, Self-Weight, Imposed Loads for Buildings*. Austrian Standards Institute: Vienna, Austria, 2011.
21. BSI. *UK National Annex to Eurocode 1: Actions on Structures—Part 1-1 (BS EN 1991-1-1:2002)*; British Standards Institution: London, UK, 2002.
22. AFNOR. *NF P 06-111-2: National Annex to NF EN 1991-1-1—Eurocode 1: Actions on Structures*; AFNOR: Paris, France, 2004.
23. Schlicke, D. Resource-responsible construction with concrete through agile structural design. In *Agile Digitalisierung im Baubetrieb: Innovative Wege zur Transformation und Best Practices*; Springer: Wiesbaden, Germany, 2023; pp. 683–699.
24. Stummer, S. Influence of Structural Stiffness on Settlement Behavior and Practical Advices. Master’s Thesis, Institute of Concrete Structures, Graz University of Technology, Graz, Austria, 2025.
25. Stopp, K. Load-Bearing and Deformation Behaviour of Large-Area Founded Reinforced Concrete Structures Considering Soil–Structure Interaction. Ph.D. Thesis, Bergische Universität Wuppertal, Wuppertal, Germany, 2010.
26. Sofistik, A.G. *SOFiSTiK Structural Analysis Software, Version 2023*; SOFiSTiK: Bavaria, Germany, 2023.
27. Brinkgreve, R.; Engin, E.; Swolfs, W. *PLAXIS 3D Reference Manual, Version 2024.3*; Bentley Systems: Delft, The Netherlands, 2024.
28. AK 2.4 “Excavations”. *Recommendations of the Working Group ‘Numerics in Geotechnics’—EANG*, 1st ed.; Ernst & Sohn: Berlin, Germany, 2014.
29. Tschuchnigg, F. 3D Finite Element Modelling of Deep Foundations Employing an Embedded Pile Formulation. Ph.D. Thesis, Graz University of Technology, Graz, Austria, 2012.
30. Von Soos, P.; Engel, J. Soil and rock properties—Their determination. In *Grundbau-Taschenbuch, Part 1*, 8th ed.; Witt, K.J., Ed.; Ernst & Sohn: Berlin, Germany, 2017; pp. 142–143.
31. Benz, T. Small-Strain Stiffness of Soils and its Numerical Consequences. Ph.D. Thesis, University of Stuttgart, Stuttgart, Germany, 2007.
32. *EN1997-1:2004; CEN Eurocode 7—Geotechnical Design, Part 1: General Rules*. European Committee for Standardization: Brussels, Belgium, 2004.
33. *EN1992-1-1:2004; CEN Eurocode 2—Design of concrete structures, Part 1-1: General rules and rules for buildings*. European Committee for Standardization: Brussels, Belgium, 2004.
34. fib. *fib Model Code for Concrete Structures 2010*; Ernst & Sohn: Berlin, Germany, 2013; ISBN 978-3-433-03061-5.
35. Wallner, C.; Tschuchnigg, F.; Schlicke, D. Limits of linear-elastic soil in soil–structure interaction. *Beton- Und Stahlbetonbau* **2025**, *120*, 484–493. [[CrossRef](#)]

**Disclaimer/Publisher’s Note:** The statements, opinions and data contained in all publications are solely those of the individual author(s) and contributor(s) and not of MDPI and/or the editor(s). MDPI and/or the editor(s) disclaim responsibility for any injury to people or property resulting from any ideas, methods, instructions or products referred to in the content.